

PAPER

A multimodal approach to estimating vigilance using EEG and forehead EOG

To cite this article: Wei-Long Zheng and Bao-Liang Lu 2017 *J. Neural Eng.* **14** 026017

View the [article online](#) for updates and enhancements.

Related content

- [Detection of lapses in responsiveness from the EEG](#)
Malik T R Peiris, Paul R Davidson, Philip J Bones et al.
- [Monitoring alert and drowsy states by modeling EEG source nonstationarity](#)
Sheng-Hsiou Hsu and Tzzy-Ping Jung
- [EEG predictors of covert vigilant attention](#)
Adrien Martel, Sven Dähne and Benjamin Blankertz

A multimodal approach to estimating vigilance using EEG and forehead EOG

Wei-Long Zheng¹ and Bao-Liang Lu^{1,2,3,4}

¹ Center for Brain-like Computing and Machine Intelligence, Department of Computer Science and Engineering, Shanghai Jiao Tong University, Shanghai, People's Republic of China

² Key Laboratory of Shanghai Education Commission for Intelligent Interaction and Cognitive Engineering, Shanghai Jiao Tong University, Shanghai, People's Republic of China

³ Brain Science and Technology Research Center, Shanghai Jiao Tong University, Shanghai, People's Republic of China

E-mail: weilong@sjtu.edu.cn and bllu@sjtu.edu.cn

Received 15 August 2016, revised 22 December 2016

Accepted for publication 10 January 2017

Published 22 February 2017



Abstract

Objective. Covert aspects of ongoing user mental states provide key context information for user-aware human computer interactions. In this paper, we focus on the problem of estimating the vigilance of users using EEG and EOG signals. **Approach.** The PERCLOS index as vigilance annotation is obtained from eye tracking glasses. To improve the feasibility and wearability of vigilance estimation devices for real-world applications, we adopt a novel electrode placement for forehead EOG and extract various eye movement features, which contain the principal information of traditional EOG. We explore the effects of EEG from different brain areas and combine EEG and forehead EOG to leverage their complementary characteristics for vigilance estimation. Considering that the vigilance of users is a dynamic changing process because the intrinsic mental states of users involve temporal evolution, we introduce continuous conditional neural field and continuous conditional random field models to capture dynamic temporal dependency. **Main results.** We propose a multimodal approach to estimating vigilance by combining EEG and forehead EOG and incorporating the temporal dependency of vigilance into model training. The experimental results demonstrate that modality fusion can improve the performance compared with a single modality, EOG and EEG contain complementary information for vigilance estimation, and the temporal dependency-based models can enhance the performance of vigilance estimation. From the experimental results, we observe that theta and alpha frequency activities are increased, while gamma frequency activities are decreased in drowsy states in contrast to awake states. **Significance.** The forehead setup allows for the simultaneous collection of EEG and EOG and achieves comparative performance using only four shared electrodes in comparison with the temporal and posterior sites.

Keywords: brain-computer interfaces, vigilance estimation, EEG, EOG, multimodal approach, temporal dependency

(Some figures may appear in colour only in the online journal)

1. Introduction

Humans interact with their surrounding complex environments based on their current states, and context awareness plays an important role during such interactions. However, the

majority of the existing systems lack this ability and generally interact with users in a rule-based fashion. Covert aspects of ongoing user mental states provide key context information in user-aware human computer interactions (Zander and Jatzev 2012), which can help systems react adaptively in a proper manner. Various studies have introduced the assessment of the mental states of users, such as intention, emotion,

⁴ Author to whom any correspondence should be addressed

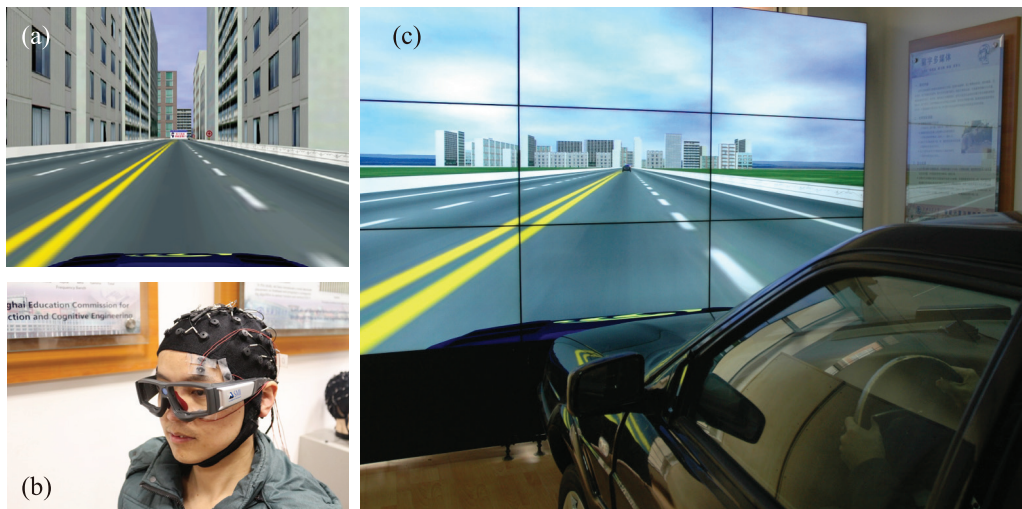


Figure 1. The simulated driving system and the experimental scene. (a) The virtual-reality-based simulated driving scenes, including various weather and roads. (b) Forehead EOG, EEG and eye movements are simultaneously recorded using the Neuroscan system and eye tracking glasses. (c) The simulated driving experiments are performed in a real vehicle without unnecessary engine and other components. During the experiments, the subjects are asked to drive the car using the steering wheel and gas pedal. The driving scenes are synchronously updated according to subjects' operations. There is no warning feedback to subjects after sleeping.

and workload, to promote active interactions between users and machines (Mühl *et al* 2014, Kang *et al* 2015, Lu *et al* 2015, Zheng and Lu 2015). Zander and Kothe proposed the concept of a passive brain-computer interface (BCI) to fuse conventional BCI systems with cognitive monitoring (Zander and Kothe 2011). It is attractive to implement these novel BCI systems with increasing information flow of human states without simultaneously increasing the cost significantly. Among these cognitive states, vigilance is a vital component, which refers to the ability to endogenously maintain focus.

Various working environments require sustained high vigilance, particularly for some dangerous occupations such as driving trucks and high-speed trains. In these cases, a decrease in vigilance (Grier *et al* 2003) or a momentary lapse of attention (Davidson *et al* 2007, Peiris *et al* 2011) might severely endanger public transportation safety. Driving fatigue is reported to be a major factor in fatal road accidents.

Various approaches for estimating vigilance levels have been proposed in the literature (Ji *et al* 2004, Dong *et al* 2011, Sahayadhas *et al* 2012). However, several research challenges still exist. Vigilance decrement is a dynamic changing process because the intrinsic mental states of users involve temporal evolution rather than a time point. This process cannot simply be treated as a function of the duration of time while engaged in tasks. The ability to predict vigilance levels with high temporal resolution is more feasible in real-world applications (Davidson *et al* 2007). Moreover, drivers' vigilance levels cannot be simply classified into several discrete categories but should be quantified in the same way as the blood alcohol level (Ranney 2008, Dong *et al* 2011). We still lack a standardized method for measuring the overall vigilance levels of humans.

Among various modalities, EEG is reported to be a promising neurophysiological indicator of the transition between wakefulness and sleep in various studies because EEG

signals directly reflect human brain activity (Berka *et al* 2007, Khushaba *et al* 2011, Shi and Lu 2013, Kim *et al* 2014, Lin *et al* 2014, Martel *et al* 2014). Rosenberg and colleagues recently presented a neuromarker for sustained attention from whole-brain functional connectivity (Rosenberg *et al* 2016). They developed a network model called the sustained attention network for predicting attentional performance. Moreover, EEG has intrinsic potential to allow fatigue detection at onset or even before onset (Davidson *et al* 2007). O'Connell and colleagues examined the temporal dynamics of EEG signals preceding a lapse of sustained attention (O'Connell *et al* 2009). Their results demonstrated that the specific neural signatures of attentional lapses are registered in the EEG up to 20s prior to an error. Lin *et al* presented a wireless and wearable EEG system for evaluating drivers' vigilance levels, and they tested their system in a virtual driving environment (Lin *et al* 2014). They also combined lapse detection and feedback efficacy assessment for implementing a closed-loop system. By monitoring the changes of EEG patterns, they were able to detect driving performance and estimate the efficacy of arousing warning feedback delivered to drowsy subjects (Lin *et al* 2013).

In addition to EEG, EOG signals contain characteristic information on various eye movements, which are often utilized to estimate vigilance because of its easy setup and high signal-noise ratio (Papadelis *et al* 2007, Damousis and Tzovaras 2008, Ma *et al* 2010, 2014). Researchers have developed various multimodal approaches for constructing hybrid BCIs (Pfurtscheller *et al* 2010) and combining brain signals and eye movements for robotic control and cognitive monitoring (Lee *et al* 2010, Ma *et al* 2014, McMullen *et al* 2014, Zheng *et al* 2014). Bulling and colleagues found that eye movements from EOG signals are good indicators for activity recognition (Bulling *et al* 2011). However, the electrodes in the traditional EOG are placed around the

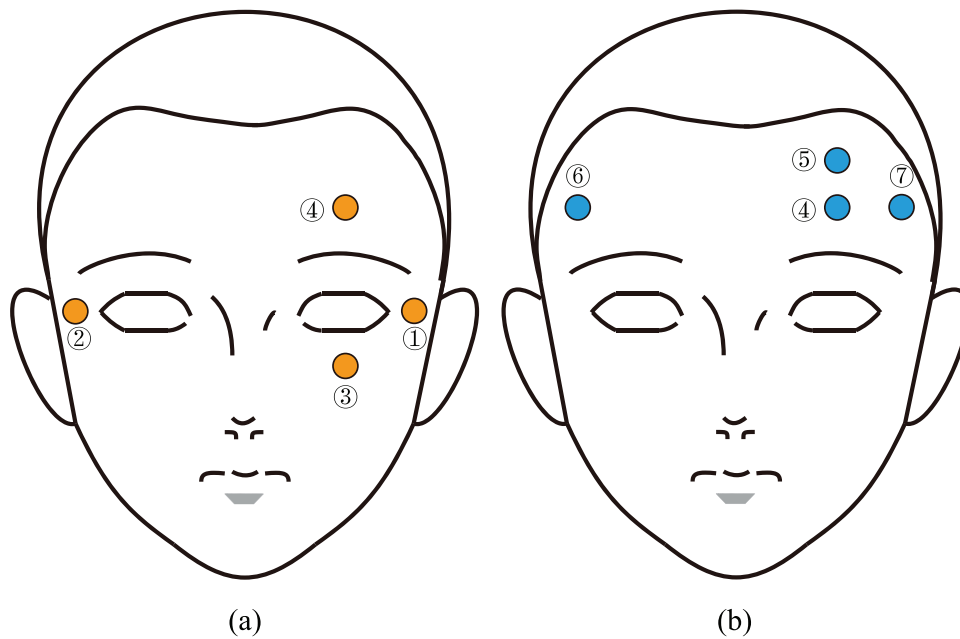


Figure 2. Electrode placements for the traditional (a) and forehead (b) EOG setups. The yellow and blue dots indicate the electrode placements of the traditional EOG and forehead EOG, respectively. Electrode four is the shared electrode of both setups.

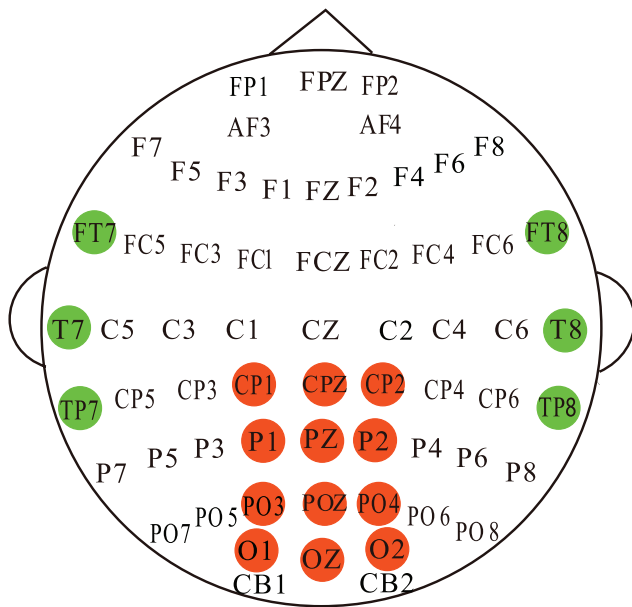


Figure 3. Electrode placements for the EEG setups. 12-channel and 6-channel EEG signals were recorded from the posterior site (red colour) and temporal site (green colour), respectively.

eyes, which may distract users and cause discomfort. In our previous study, we proposed a new electrode placement on the forehead and extracted various eye movement features from the forehead EOG (Zhang *et al* 2015a, Huo *et al* 2016). Various studies have indicated that signals from different modalities represent different aspects of covert mental states (Calvo and D’Mello 2010, Sahayadhas *et al* 2012, D’mello and Kory 2015). EEG and EOG represent internal cognitive states and external subconscious behaviours, respectively. These two modalities contain complementary information and can be integrated to construct a more robust vigilance estimation model.

2. Methods

2.1. Experiment setup

To collect EEG and EOG data, we developed a simulated driving system. A four-lane highway scene is shown on a large LCD screen in front of a real vehicle without the unnecessary engine and other components. The vehicle movements in the software are controlled by the steering wheel and gas pedal, and the scenes are simultaneously updated according to the participants’ operations. The road is primarily straight and monotonous to induce fatigue in the subjects more easily. The simulated driving system and the experimental scene are shown in figure 1.

A total of 23 subjects (mean age: 23.3, STD: 1.4, 12 females) participated in the experiments. All participants possessed normal or corrected-to-normal vision. Caffeine, tobacco, and alcohol were prohibited prior to participating in the experiments. At the beginning of the experiments, a short pre-test was performed to ensure that every participant understood the instructions. Most experiments were performed in the early afternoon (approximately 13:30) after lunch to induce fatigue easily when the circadian rhythm of sleepiness reached its peak (Ferrara and De Gennaro 2001). The duration of the entire experiment was approximately 2h. The participants were asked to drive the car in the simulated environments without any alertness.

Both EEG and forehead EOG signals were recorded simultaneously using the Neuroscan system with a 1000 Hz sampling rate. The electrode placement of the forehead EOG (Zhang *et al* 2015a) is shown in figure 2(b). For the EEG setup, we recorded 12-channel EEG signals from the posterior site (CP1, CPZ, CP2, P1, PZ, P2, PO3, POZ, PO4, O1, OZ, and O2) and 6-channel EEG signals from the temporal site (FT7, FT8, T7, T8, TP7, and TP8) according to the international 10–20 electrode system shown in figure 3. Eye movements



Figure 4. The SMI eye tracking glasses used in this study and the pupillary image captured in one experiment.

were simultaneously recorded using SMI ETG eye tracking glasses⁵, and the facial video was recorded from a video camera mounted in front of the participants.

For reproducing the results in this paper and enhancing cooperation in related research fields, the dataset used in this study will be freely available to the academic community as a subset of SEED⁶.

2.2. Vigilance annotations

The primary challenge of vigilance estimation using a supervised machine learning paradigm is how to quantitatively label the sensor data because the ground truth of convert mental states cannot be accurately obtained in theory. To date, researchers have proposed various vigilance annotation methods in the literature, such as lane departure and local error rates (Makeig and Inlow 1993, Wang *et al* 2015). Lin *et al* designed an event-related lane-departure driving task in which the subjects were asked to respond to the random drifts as soon as possible and the response time reflected the vigilance states of the subjects (Lin *et al* 2010, 2013). Shi and Lu (2013) conducted a study in which the local error rate of the subjects' performance was used as the vigilance measurement. The subjects were asked to press correct buttons according to the colours of traffic signs. These two annotation methods are based on subjects' behaviours and can reflect their actual vigilance levels to some extent. However, they are not feasible for dual tasks, particularly in real-world driving environments.

There is another annotation method called PERCLOS (Dinges and Grace 1998), which refers to the percentage of eye closure. It is one of the most widely accepted vigilance indices in the literature (Bergasa *et al* 2006, Dong *et al* 2011, Trutschel *et al* 2011). Conventional driving fatigue detection methods utilize facial videos to calculate the PERCLOS index. However, the performance of facial videos can be influenced by environmental changes, especially for various illuminations and heavy occlusion. In this study, we adopt an automatic continuous vigilance annotation method using eye tracking glasses, which was proposed in our previous work (Gao *et al* 2015). This approach allows vigilance to be measured in both laboratory and real-world environments.

Compared with facial videos, eye tracking glasses can more precisely capture different eye movements, such as blink,

fixation, and saccade, as shown in figure 4. The eye tracking-based PERCLOS index can be calculated from the percentage of the durations of blinks and 'CLOS' over a specified time interval as follows:

$$\text{PERCLOS} = \frac{\text{blink} + \text{CLOS}}{\text{interval}}, \text{ and} \quad (1)$$

$$\text{interval} = \text{blink} + \text{fixation} + \text{saccade} + \text{CLOS}, \quad (2)$$

where 'CLOS' denotes the duration of the eye closures.

We evaluated the efficiency of the eye tracking-based method for vigilance annotations with the facial videos recorded simultaneously and found a high correlation between the PERCLOS index and the subject's current cognitive states. Compared with other approaches (Shi and Lu 2010, Ma *et al* 2014, Wang *et al* 2015), this method is more feasible for real-world driving environments, where performing dual tasks can distract attention and cause safety issues (Oken and Salinsky 2007). This new vigilance annotation method can be performed automatically without too much interference to the drivers.

Note that although the eye tracking-based approach can estimate the vigilance level more precisely, it is not currently feasible to apply it to real-world applications due to its very expensive cost. Here, we utilize eye tracking glasses as a vigilance annotation device to obtain more accurate labelled EEG and EOG data for training vigilance estimation models.

2.3. Feature extraction

2.3.1. Preprocessing for forehead EOG.

For traditional EOG recordings, the electrodes are mounted around the eyes using the electrodes numbered one to four in figure 2(a). However, in real-world applications, such electrode placement is not easily mounted and may distract users with discomfort. To implement wearable devices for real-world vigilance estimation, we propose placing all the electrodes on the forehead, as shown in figure 2(b), and separating vertical EOG (VEO) and horizontal EOG (HEO) using the electrodes numbered four to seven shown in figure 2(b). For the traditional EOG setup shown in figure 2(a), the VEO and HEO signals are obtained by subtracting electrodes four and three and electrodes one and two, respectively. VEO and HEO signals contain details of eye movements, such as blink, saccade, and fixation.

How to extract VEO and HEO signals from the forehead EOG setup is one of the key problems in this study. We

⁵ <http://eyetracking-glasses.com/>

⁶ <http://bcmi.sjtu.edu.cn/~seed/>

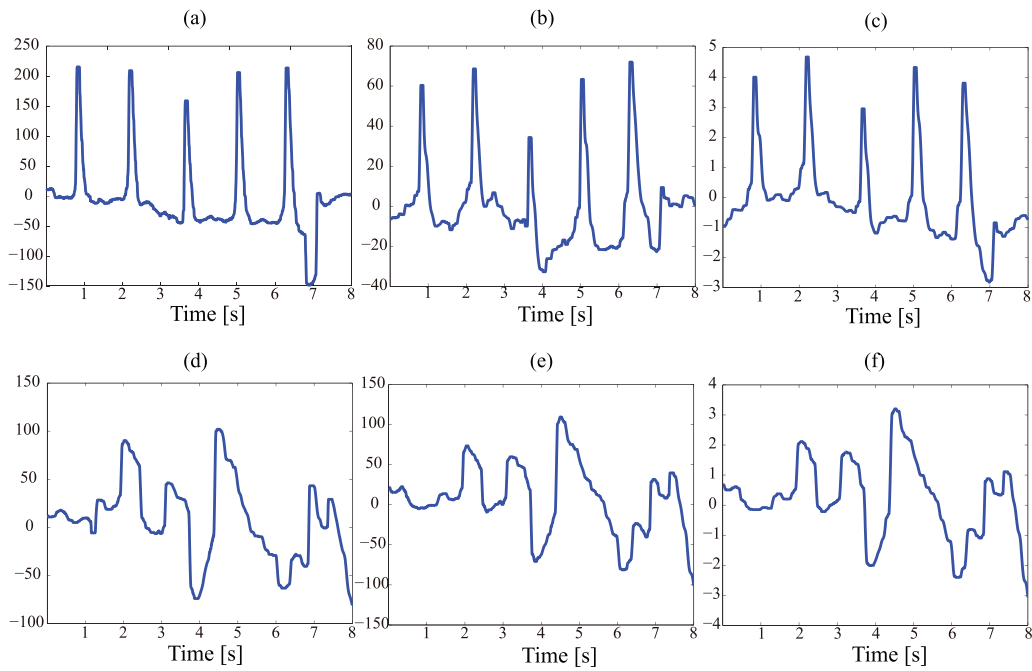


Figure 5. Comparison of traditional EOG and forehead EOG using minus operation and ICA separation strategies. Here, (a) and (d) are traditional VEO and HEO; (b) and (e) are extracted VEO_f and HEO_f from forehead EOG using the minus operation; and (c) and (f) are extracted VEO_f and HEO_f from forehead EOG using the ICA approach.

extracted VEO_f signals from electrodes numbered four and seven and extracted HEO_f signals from electrodes five and six using two separation strategies: the minus rule and independent component analysis (ICA). For the minus rule, the subtraction of channels five and seven is an approximation of VEO, named VEO_f, and the subtraction of channels five and six is an approximation of HEO, named HEO_f. Here, the subscript ‘f’ indicates ‘forehead’.

ICA is a blind source separation method proposed to decompose a multivariate signal into independent non-Gaussian signals (Delorme and Makeig 2004). We extracted the VEO_f and HEO_f components using FASTICA (Delorme and Makeig 2004) from channels four and seven and channels five and six, respectively. The comparison of the traditional EOG and forehead EOG using the minus operation and ICA separation strategies is depicted in figure 5. As shown, the extracted VEO_f and HEO_f from the forehead electrodes have similar waves to the traditional ones, and the forehead VEO_f and HEO_f can capture critical eye movements, such as blinks and saccades.

2.3.2. Feature extraction from forehead EOG. After preprocessing forehead EOG signals and extracting VEO_f and HEO_f, we detected eye movements such as blinks and saccades using the wavelet transform method (Bulling *et al* 2011). We computed the continuous wavelet coefficients at a scale of 8 with a Mexican hat wavelet defined by

$$\psi(t) = \frac{2}{\sqrt{3\sigma\pi^4}} \left(1 - \frac{t^2}{\sigma^2}\right) e^{-\frac{t^2}{2\sigma^2}}, \quad (3)$$

where σ is the standard deviation. Because the wavelet transform is sensitive to singularities, we used the peak detection

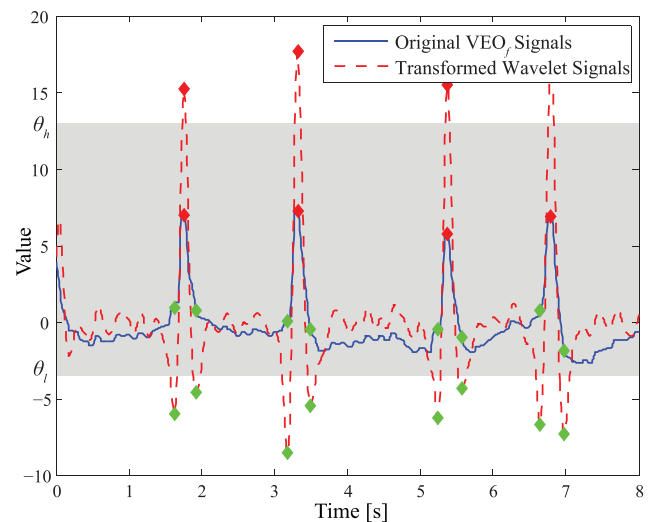


Figure 6. The blink detected by using continuous wavelet transform. We applied two thresholds θ_h and θ_l on the transformed wavelet signals and detected peaks to locate blink segments. Red markers indicate the peaks of each blink, and green markers indicate the start and end points of each blink.

algorithm on the wavelet coefficients to detect blinks and saccades from the forehead VEO_f and HEO_f, respectively. The detected blinks and saccades are shown in figures 6 and 7, respectively.

By applying thresholds on the continuous wavelet coefficients, we encoded the positive and negative peaks in forehead VEO_f and HEO_f into sequences, where the positive peak was encoded as ‘1’ and the negative one as ‘0’. A saccade is characterized by a sequence of two successive positive and

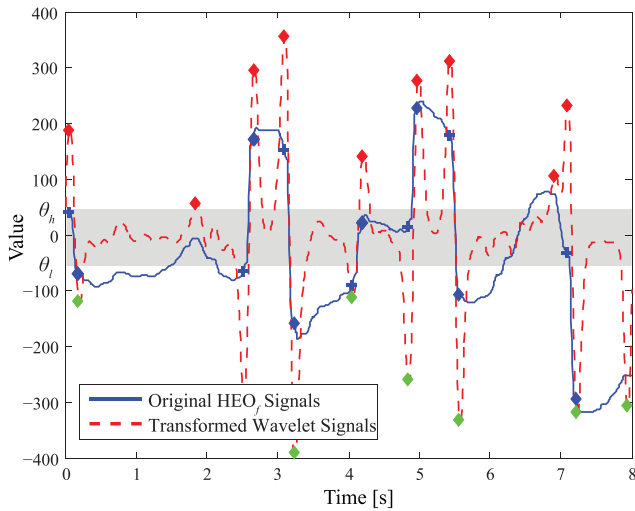


Figure 7. The saccade detected by using continuous wavelet transform. Similar to blink detection, we applied two thresholds θ_h and θ_l on the transformed wavelet signals and used peak detection on the transformed wavelet signals. Blue cross markers and diamond markers indicate the start and end points of each saccade, respectively.

negative peaks in the coefficients. A blink contains three successive large peaks, namely, negative, positive, and negative, and the time between two positive peaks should be smaller than the minimum time. Therefore, for the encoding, segments with ‘01’ or ‘10’ are recognized as saccade candidates, and segments with ‘010’ are recognized as blink candidates. Moreover, there are some other constraints, such as slope, correlation, and maximal segment length, for guaranteeing a precise detection of blinks and saccades. Following the detection of blinks and saccades, we extracted the statistical parameters, such as the mean, maximum, variance, and derivative, of different eye movements with an 8 s non-overlapping window as the EOG features. We extracted a total of 36 EOG features from the detected blinks, saccades, and fixations. Table 1 presents the details of the extracted 36 eye movement features.

2.3.3. Forehead EEG signal extraction. For conventional EEG-based approaches, the EOG signals are always considered to be severe contamination, particularly for frontal sites. Many methods have been proposed for removing eye movement and blink artifacts from EEG recordings (Delorme and Makeig 2004, Daly *et al* 2015, Urigüen and Garcia-Zapirain 2015). However, in this study, we consider that both EEG and EOG contain discriminative information for vigilance estimation. Our intuitive concept is that it is possible to separate EEG and EOG signals from the shared forehead electrodes. The main advantage of this concept is that we can leverage the favourable properties of both EEG and EOG modalities while simultaneously not increasing the setup cost.

We utilize the FASTICA algorithm to extract EEG and EOG components from the four forehead channels (Nos. 4–7) shown in figure 2(b). The ICA algorithm decomposes the multi-channel data into a sum of independent components (Jung *et al* 2000). Similar to artifact removal using blind signal separation in conventional approaches, the forehead EEG signals are reconstructed with a weight matrix by discarding the EOG

components. The raw data recorded at the four forehead channels (Nos. 4–7) are concatenated as the input matrix X for ICA as follows:

$$X = [Ch_4; Ch_5; -Ch_6; Ch_7], \quad (4)$$

where the rows of the input matrix X are signals Ch_4 , Ch_5 , $-Ch_6$, and Ch_7 from channels Nos. 4–7. After ICA decomposition, the un-mixing matrix W can be obtained, which decomposes the multi-channel data into a sum of independent components as follows:

$$U = W * X, \quad (5)$$

where the rows of U are time courses of activations of the ICA components. The columns of the inverse matrix W^{-1} indicate the projection strengths of the corresponding components. Therefore, the clean forehead EEG signals can be derived as

$$\tilde{X} = W^{-1} * \tilde{U}, \quad (6)$$

where \tilde{U} is the matrix of activation waveforms U with rows representing EOG components set to zero.

The decomposed independent components and reconstructed forehead EEG of one segment under eye closure conditions are shown in figure 8. Under eye closure conditions, the alpha rhythm appears more dominant in EEG signals in previous studies (Papadelis *et al* 2007). From figure 8(a), we can observe that the first two rows are the corresponding eye movement components, and the last two rows contain EEG components with high alpha power values. The reconstructed signals contain characteristics of EEG waves, which are accompanied by high alpha bursts. The results presented in figure 8 demonstrate the efficiency of our approach in extracting EEG signals from forehead electrodes.

2.3.4. Feature extraction from EEG. In addition to forehead EOG, we recorded EEG data from temporal and posterior sites, which showed high relevance along with vigilance in the literature and our previous work (Khushaba *et al* 2011, Shi and Lu 2013). For preprocessing, the raw EEG data were processed with a band-pass filter between 1 and 75 Hz to reduce artifacts and noise and downsampled to 200 Hz to reduce the computational complexity. For feature extraction, an efficient EEG feature called differential entropy (DE) was proposed for vigilance estimation and emotion recognition (Duan *et al* 2013, Shi *et al* 2013), which showed superior performance compared to the conventional power spectral density features.

The original formula for calculating differential entropy is defined as

$$h(X) = - \int_X f(x) \log(f(x)) dx. \quad (7)$$

If a random variable obeys the Gaussian distribution $N(\mu, \sigma^2)$, the differential entropy can simply be calculated by the following formulation,

$$h(X) = - \int_{-\infty}^{\infty} f(x) \log(f(x)) dx = \frac{1}{2} \log 2\pi e \sigma^2, \quad (8)$$

where $f(x) = \frac{1}{\sqrt{2\pi\sigma^2}} \exp\left(-\frac{(x-\mu)^2}{2\sigma^2}\right)$.

Table 1. The details of the extracted 36 eye movement features.

Group	Extracted features
Blink	Maximum/mean/sum of blink rate maximum/minimum/mean of blink amplitude, mean/maximum of blink rate variance and amplitude variance power/mean power of blink amplitude blink numbers
Saccade	Maximum/minimum/mean of saccade rate and saccade amplitude, maximum/mean of saccade rate variance and amplitude variance, power/mean power of saccade amplitude, saccade numbers
Fixation	mean/maximum of blink duration variance and saccade duration variance maximum/minimum/mean of blink duration and saccade duration

According to the DE definition mentioned above, for each EEG segment, we extracted the DE features from five frequency bands: delta (1–4 Hz), theta (4–8 Hz), alpha (8–14 Hz), beta (14–31 Hz), and gamma (31–50 Hz). We also extracted the DE features from the total frequency band (1–50 Hz) with a 2 Hz frequency resolution. All the DE features were calculated using short-term Fourier transforms with an 8 s non-overlapping window.

2.4. Vigilance estimation

After obtaining vigilance labels and EOG/EEG features, we used support vector regression (SVR) with radial basis function (RBF) kernels as a basic regression model. The optimal values of the parameters c and g were tuned with the grid search. As the modality fusion strategy, we used feature-level fusion, in which the feature vectors of EEG and EOG are directly concatenated into a larger feature vector as inputs. For evaluation, we separated the entire data from one experiment into five sessions and evaluated the performance with 5-fold cross validation. There are a total of 885 samples for each experiment.

The root mean square error (RMSE) and correlation coefficient (COR) are the most commonly used evaluation metrics for continuous regression models (Nicolaou *et al* 2011). RMSE is the squared error between the prediction and the ground truth, and it is defined as follows:

$$\text{RMSE}(Y, \hat{Y}) = \sqrt{\frac{1}{N} \sum_{i=1}^N (y_i - \hat{y}_i)^2}, \quad (9)$$

where $Y = (y_1, y_2, \dots, y_N)^T$ is the ground truth and $\hat{Y} = (\hat{y}_1, \hat{y}_2, \dots, \hat{y}_N)^T$ is the prediction.

Since RMSE-based evaluation cannot provide structural information, we used COR to overcome the shortcomings of RMSE. COR provides an evaluation of the linear relationship between the prediction and the ground truth, which reflects the consistency of their trends. Pearson's correlation coefficient is defined as follows:

$$\text{COR}(Y, \hat{Y}) = \frac{\sum_{i=1}^N (y_i - \bar{y})(\hat{y}_i - \bar{\hat{y}})}{\sqrt{\sum_{i=1}^N (y_i - \bar{y})^2 \sum_{i=1}^N (\hat{y}_i - \bar{\hat{y}})^2}}, \quad (10)$$

where \bar{y} and $\bar{\hat{y}}$ are the means of Y and \hat{Y} . However, COR is sensitive to short segments and is appropriate for long evaluation metrics. Therefore, we concatenated the predictions and ground truth of five sessions and calculated COR as the final evaluation. In general, the more accurate the model is, the higher the COR is and the lower the RMSE is.

2.5. Incorporating temporal dependency into vigilance estimation

Vigilance is a dynamic changing process because the intrinsic mental states of users involve temporal evolution. To incorporate the temporal dependency into vigilance estimation, we introduced continuous conditional neural field (CCNF) and continuous conditional random field (CCRF) when constructing vigilance estimation models. CCNF and CCRF are extensions of conditional random field (CRF) (Lafferty *et al* 2001) for continuous variable modelling that incorporates temporal or spatial information and have shown promising performance in various applications (Baltrušaitis *et al* 2013, Baltrušaitis *et al* 2014, Imbrasaite *et al* 2014). CCNF combines the nonlinearity of conditional neural fields (Peng *et al* 2009) and the continuous output of CCRF.

The probability distribution of CCNF for a particular sequence is defined as follows:

$$P(\mathbf{y}|\mathbf{x}) = \frac{\exp(\Psi)}{\int_{-\infty}^{\infty} \exp(\Psi) d\mathbf{y}}, \quad (11)$$

where $\int_{-\infty}^{\infty} \exp(\Psi) d\mathbf{y}$ is the normalization function, $\mathbf{x} = \{x_1, x_2, \dots, x_n\}$ is a set of input observations, $\mathbf{y} = \{y_1, y_2, \dots, y_n\}$ is a set of output variables, and n is the length of the sequence.

There are two types of features defined in these models: vertex features f_k and edge features g_k . The potential function Ψ is defined as follows:

$$\Psi = \sum_i \sum_{k=1}^{K_1} \alpha_k f_k(y_i, \mathbf{x}_i, \boldsymbol{\theta}_k) + \sum_{i,j} \sum_{k=1}^{K_2} \beta_k g_k(y_i, y_j), \quad (12)$$

where $\alpha_k > 0$, $\beta_k > 0$, the vertex features f_k denote the mapping from \mathbf{x}_i to y_i with a one-layer neural network, and $\boldsymbol{\theta}_k$ is the weight vector for the neuron k .

The vertex features of CCNF are defined as

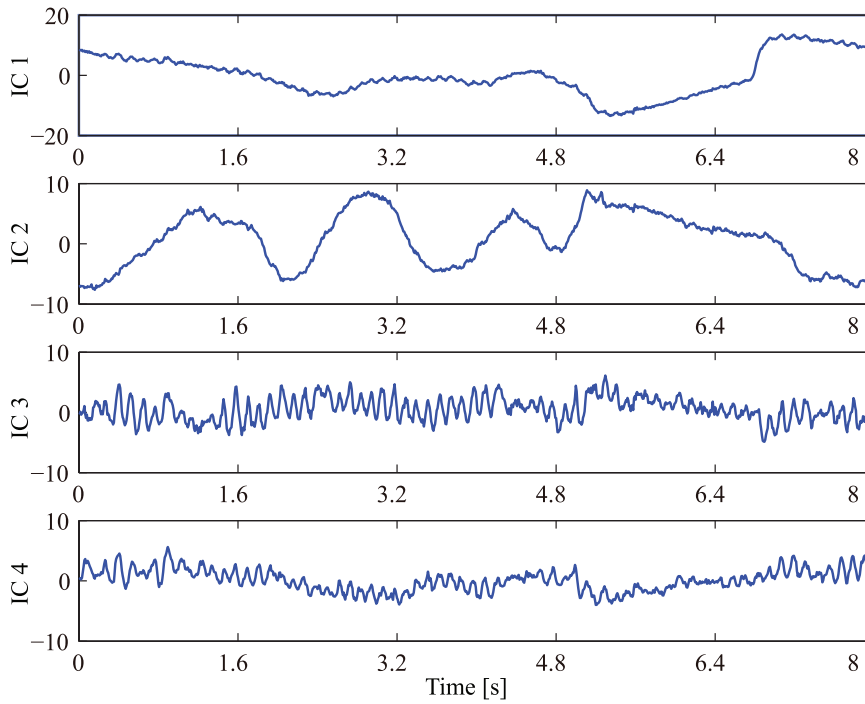
$$f_k(y_i, \mathbf{x}_i, \boldsymbol{\theta}_k) = -(y_i - h(\boldsymbol{\theta}_k, \mathbf{x}_i))^2, \quad \text{and} \quad (13)$$

$$h(\boldsymbol{\theta}, \mathbf{x}_i) = \frac{1}{1 + e^{-\boldsymbol{\theta}^T \mathbf{x}_i}}, \quad (14)$$

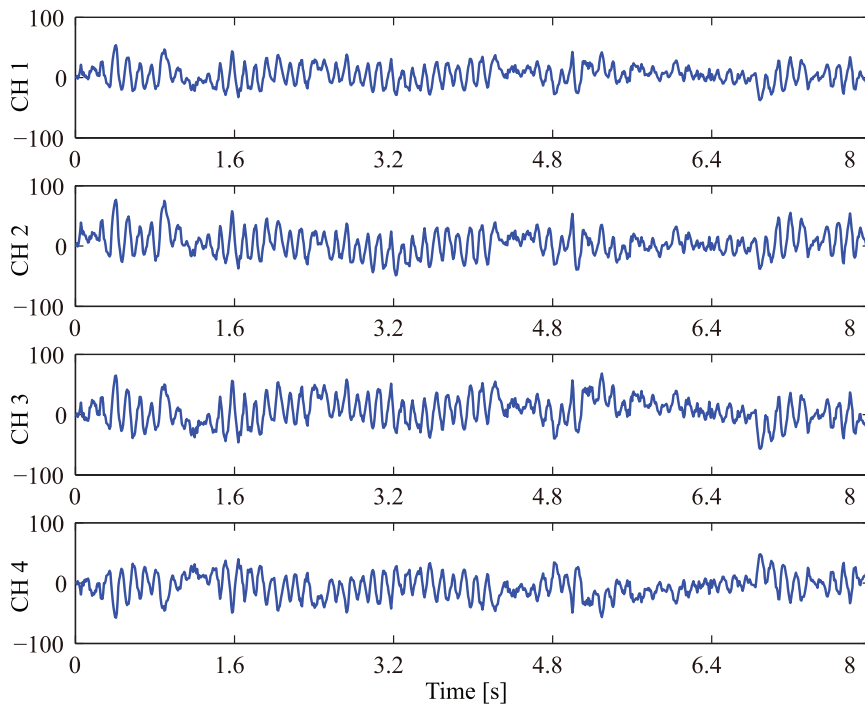
where the optimal number of vertex features K_1 is tuned with cross-validation. In our experiments, we evaluated $K_1 = \{10, 20, 30\}$.

The edge features g_k denote the similarities between observations y_i and y_j , which are defined as

$$g_k(y_i, y_j) = -\frac{1}{2} S_{i,j}^{(k)} (y_i - y_j)^2, \quad (15)$$



(a)



(b)

Figure 8. (a) The decomposed independent components from the four forehead channels (Nos. 4–7) using ICA. IC 1 and IC 2 are EOG components for eye activities. (b) The reconstructed forehead EEG by filtering out the EOG components. It can be observed that strong alpha activities are verified under eye closure conditions.

where the similarity measure $S^{(k)}$ controls the existence of the connections between two vertices.

In the experiments, K_2 is set to 1 and $S^{(k)}$ is set to 1 when two nodes i and j are neighbours; otherwise, it is 0. The sequence length n is set to seven. The formulas for

CCRF are the same as those for CCNF, except for the definition of vertex features. The vertex features of CCRF are defined as

$$f_k(y_i, \mathbf{x}_{i,k}) = -(y_i - \mathbf{x}_{i,k})^2. \quad (16)$$

Table 2. The mean RMSE, the mean COR, and their standard deviations with different separation methods. Here, the numbers in the first and second rows are the averages and standard deviations, respectively.

ICA-MINUS		EOG-ICA		EOG-MINUS	
COR	RMSE	COR	RMSE	COR	RMSE
0.7773	0.1188	0.4774	0.1582	0.7193	0.1288
0.1745	0.0391	0.5381	0.0844	0.3492	0.0588

Table 3. The average and standard deviations of COR and RMSE for different EEG features. Here, the numbers in the first and second rows are the averages and standard deviations, respectively.

(a) COR					
Posterior		Temporal		Forehead	
2 Hz	5 Bands	2 Hz	5 Bands	2 Hz	5 Bands
0.7001	0.6807	0.6678	0.6410	0.6502	0.5749
0.2250	0.2129	0.2349	0.2246	0.2116	0.2463
(b) RMSE					
Posterior		Temporal		Forehead	
2 Hz	5 Bands	2 Hz	5 Bands	2 Hz	5 Bands
0.1327	0.1429	0.1385	0.1603	0.1463	0.1640
0.0303	0.0393	0.0343	0.0722	0.0383	0.0483

The training of parameters in CCRF and CCNF is based on the conditional log-likelihood $P(\mathbf{y}|\mathbf{x})$ as a multivariate Gaussian. For more details regarding the learning and inference of CCRF and CCNF, please refer to Baltrušaitis *et al* (2014) and Imbrasaitė *et al* (2014). The outputs of support vector regression are used to train CCRF, and the original multi-dimensional features are used to train CCNF. The CCRF and CCNF regularization hyper-parameters for α_k and β_k are chosen based on a grid search in $10^{[0,1,2]}$ and $10^{[-3,-2,-1,0]}$ using the training set, respectively.

3. Experimental results

3.1. Forehead EOG-based vigilance estimation

First, we evaluated the similarity between forehead EOG and traditional EOG and the performance of forehead EOG-based vigilance estimation for different separation strategies. We extracted forehead VEO_f and HEO_f using the minus and ICA separation approaches and computed the correlation with traditional VEO and HEO. The mean correlation coefficients of VEO_f-MINUS, VEO_f-ICA, HEO_f-MINUS, and HEO_f-ICA are 0.63, 0.80, 0.81, and 0.75, respectively. These comparative results demonstrate that the extracted forehead VEO_f and HEO_f contain most of the principal information of traditional EOG.

The mean RMSE, the mean COR and their standard deviations for different separation methods are presented in table 2. ‘ICA-MINUS’ denotes ICA-based VEO_f and minus-based HEO_f separations, and it has the highest correlation coefficient with traditional VEO and HEO. As shown in table 2, ICA-MINUS achieves the best performance for

vigilance estimation in terms of both COR and RMSE. It is consistent with the above results that VEO_f-ICA and HEO_f-MINUS are more similar to the original VEO and HEO. For VEO, it contains many blink components, such as impulses, which are more likely to be detected by ICA. In contrast, the minus method reduces the amplitude of VEO signals since the polarity of the pair electrodes is the same. For HEO, saccade components are more difficult to be detected by ICA, and the polarity of the pair electrodes is different.

3.2. EEG-based vigilance estimation

We reconstructed the frontal 4-channel EEG from the forehead signals based on the ICA algorithm. In the experiments, we also recorded 12-channel and 6-channel EEG signals from posterior and temporal sites. We extracted the DE features in two ways: one is from the five frequency bands, and the other is to use a 2 Hz frequency resolution in the entire frequency band. The mean COR, mean RMSE and their standard deviations of different EEG features from different brain areas are shown in table 3. The ranking of the performance for EEG-based vigilance estimation from different brain areas is as follows: posterior, temporal, and forehead sites. For the single EEG modality, the posterior EEG contains the most critical information for vigilance estimation, which is consistent with previous findings (Khushaba *et al* 2011, Shi and Lu 2013). The EEG features with a 2 Hz frequency resolution achieve better performance than those with five frequency bands. In the later experimental evaluation in this paper, we employ the EEG features with a 2 Hz frequency resolution of the entire frequency band.

In addition to the accuracy that we discussed above for decoding brain states, another important concern is to examine whether patterns of brain activity under different cognitive states exist and whether these patterns are to some extent common across individuals. Identifying the specific relationship between brain activities and cognitive states provides evidence and support for understanding the information processing mechanism of the brain and brain state decoding (Haynes and Rees 2006). Huang *et al* demonstrated the specific links between changes in EEG spectral power and reaction time during sustained-attention tasks (Huang *et al* 2009). They found that significant tonic power increases occurred in the alpha band in the occipital and parietal areas as reaction time increased. Ray and colleagues proposed that alpha activities of EEG reflect attentional demands and that beta activities reflect emotional and cognitive processes (Ray and Cole 1985). They found increasing parietal alpha activities for tasks that do not require attention.

In this work, to investigate the changes in neural patterns associated with vigilance, we split the EEG data into three categories (awake, tired, and drowsy) with two thresholds (0.35 and 0.7) according to the PERCLOS index. We averaged the DE features over different experiments. Figure 9 presents the mean neural patterns of awake and drowsy states as well as the difference between them. As shown in figure 9, increasing theta and alpha frequency activities and decreasing gamma frequency activities exist in temporal and parietal areas in drowsy states in contrast to awake states ($p < 0.01$, one-way analysis of variance, ANOVA).

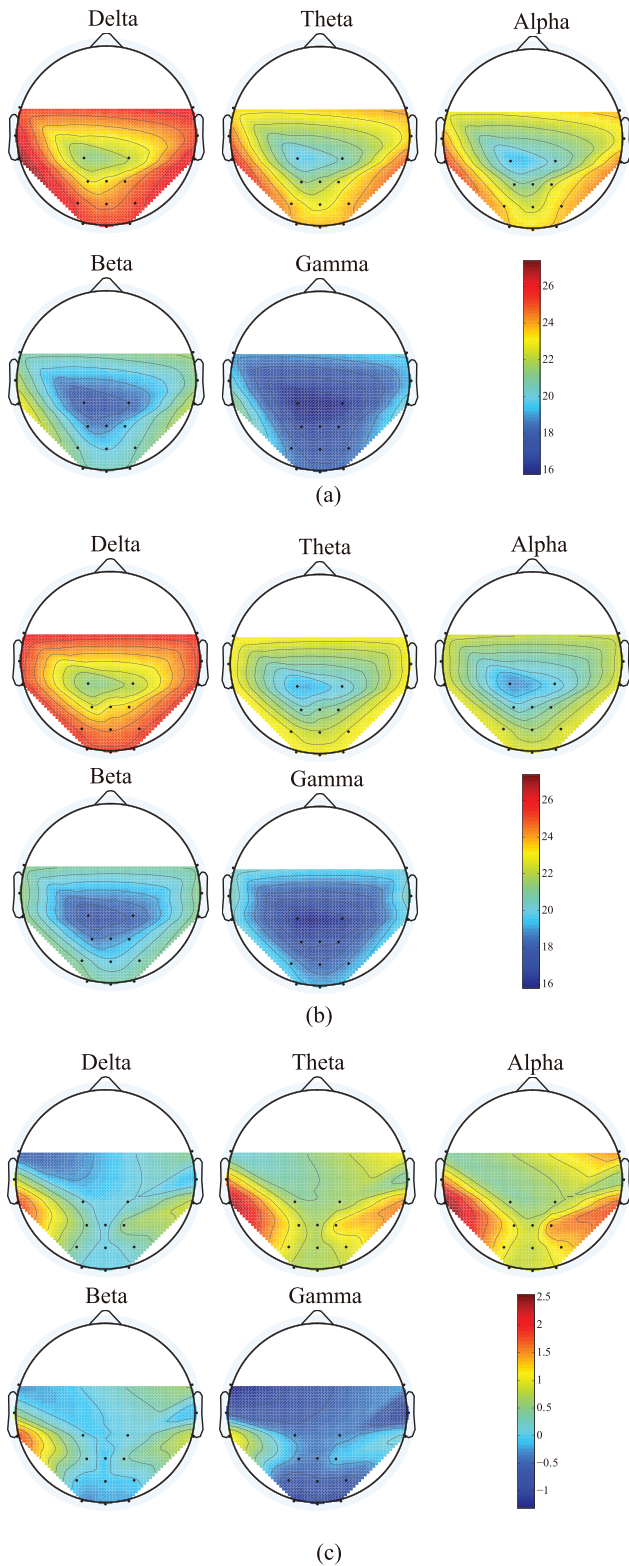


Figure 9. The mean neural patterns of awake (a) and drowsy (b) states as well as the difference (c) between these two states. By applying two thresholds (0.35 and 0.7) to the PERCLOS index, we split the EEG data into three categories: awake, tired, and drowsy. From the average neural patterns, we observe that drowsy states have higher theta and alpha frequency activities and lower gamma frequency activities in temporal and parietal areas ($p < 0.01$, ANOVA).

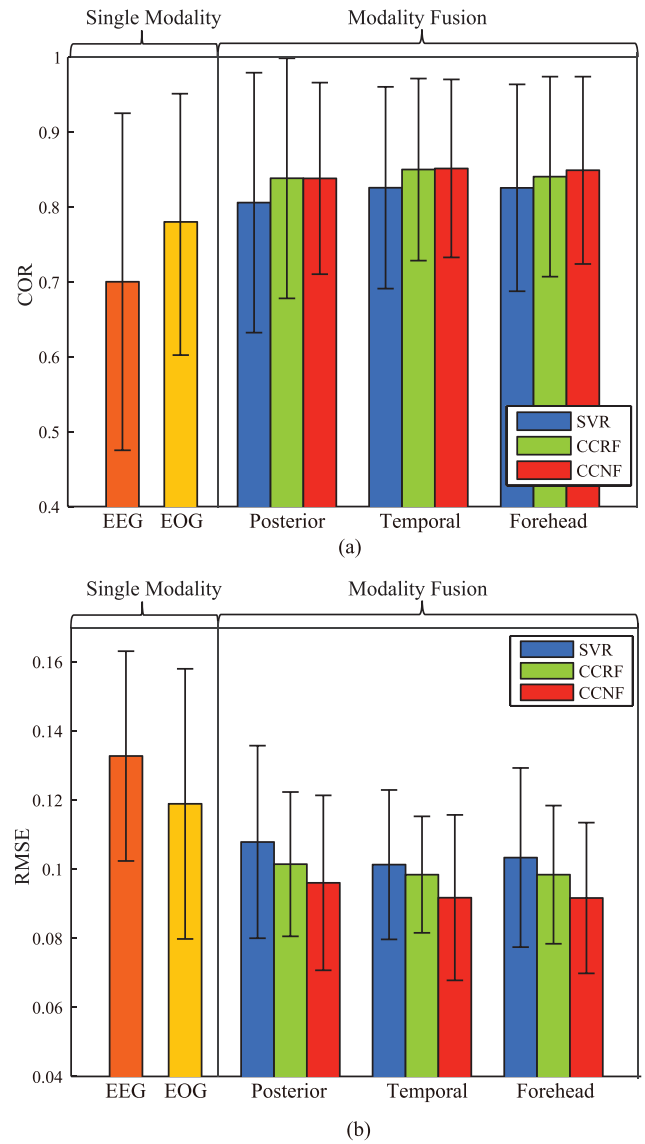


Figure 10. The mean COR (a) and mean RMSE (b) of each single modality and different modality fusion strategies.

These results are consistent with previous findings in the literature (Ray and Cole 1985, Davidson *et al* 2007, Huang *et al* 2009, O’Connell *et al* 2009, Peiris *et al* 2011, Lin *et al* 2013, Martel *et al* 2014) and support the previous evidence that the increasing trend for the ratio of slow and fast waves of EEG activities reflects decreasing attentional demands (Jap *et al* 2009).

3.3. Modality fusion with temporal dependency

In this section, we introduced a multimodal vigilance estimation approach with the fusion of EEG and forehead EOG. We combined the EEG signals from different sites (forehead, temporal, and posterior) and forehead EOG signals to utilize their complementary characteristics for vigilance estimation. The performance of each single modality and different modality fusion strategies are shown in

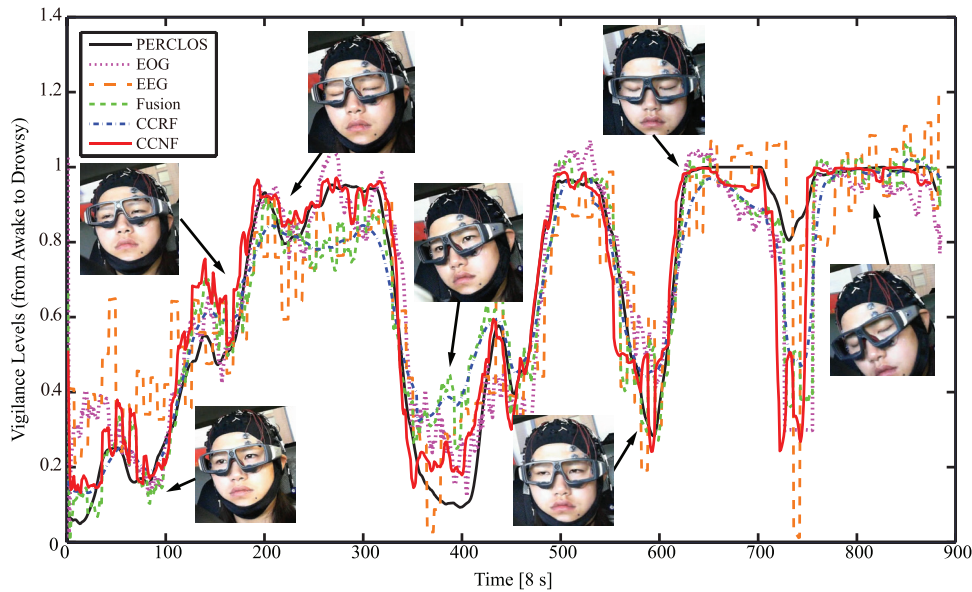


Figure 11. The continuous vigilance estimation of different methods in one experiment. As shown, the predictions from our proposed approaches are almost consistent with the true subjects' behaviours and cognitive states.

figure 10. For a single modality, forehead EOG achieves better performance than posterior EEG ($p = 0.2003$ for COR and $p = 0.1866$ for RMSE, ANOVA). The reason for this result is that forehead EOG has more information in common with the annotations of eye tracking data. Modality fusion can significantly enhance the regression performance in comparison with a single modality with a higher COR and lower RMSE. We evaluated the statistical significance using one-way analysis of variance, and the p values of COR for forehead EOG and posterior EEG are 0.2978 and 0.0264, respectively. The p values of RMSE for forehead EOG and posterior EEG are 0.0654, and 0.0002, respectively.

For different brain areas, an interesting observation is that the fusion of forehead EOG and forehead EEG achieves better performance than that of forehead EOG and posterior EEG, whereas for single EEG, the posterior site achieves the best performance. These results indicate that forehead EEG and forehead EOG have more coherent information. The temporal EEG performs slightly better than the forehead EEG. However, the former requires six extra electrodes for the setup. The forehead setup only uses four shared electrodes and both EOG and EEG features can be extracted. Therefore, the information flow can be increased without any additional setup cost. From the above discussion, we see that the forehead approach is preferred for real-world applications.

To incorporate temporal dependency information into vigilance estimation, we adopted CCRF and CCNF in this study. As shown in figures 10(a) and (b), the temporal dependency models can enhance the performance. For the forehead setup, the mean COR/RMSE of SVR, CCRF, and CCNF are 0.83/0.10, 0.84/0.10, and 0.85/0.09, respectively. The CCNF achieves the best performance with higher accuracies and lower standard deviations.

To verify whether the predictions from our proposed approaches are consistent with the true subjects' behaviours and cognitive states, the continuous vigilance estimation of one experiment is shown in figure 11. The snapshots in figure 11 show the frames corresponding to different vigilance levels. We can observe that our proposed multimodal approach with temporal dependency can moderately predict the continuous vigilance levels and its trends.

To further investigate the complementary characteristics of EEG and EOG, we analysed the confusion matrices of each modality, which reveals the strength and weakness of each modality. We split the EEG data into three categories, namely, awake, tired and drowsy states, with thresholds according to the corresponding PERCLOS index as described above. Figure 12 presents the mean confusion graph of forehead EOG and posterior EEG of all experiments. These results demonstrate that posterior EEG and forehead EOG have important complementary characteristics. Forehead EOG has the advantage of classifying awake and drowsy states (77%/76%) compared to the posterior EEG (65%/72%), whereas posterior EEG outperforms forehead EOG in recognizing tired states (88% versus 84%). The forehead EOG modality achieves better performance than the posterior EEG overall. This result may be because our ground truth labels are obtained with eye movement parameters from eye tracking glasses. The forehead EOG contains more similar information with the experimental observations. Moreover, awake states and tired states are often misclassified with each other, and similar results are observed for drowsy and tired states. In contrast, awake states are seldom misclassified as drowsy states and vice versa for both modalities. These observations are consistent with our intuitive knowledge. EEG and EOG features of awake and drowsy states should have larger differences. These results indicate that EEG and EOG have different discriminative powers for

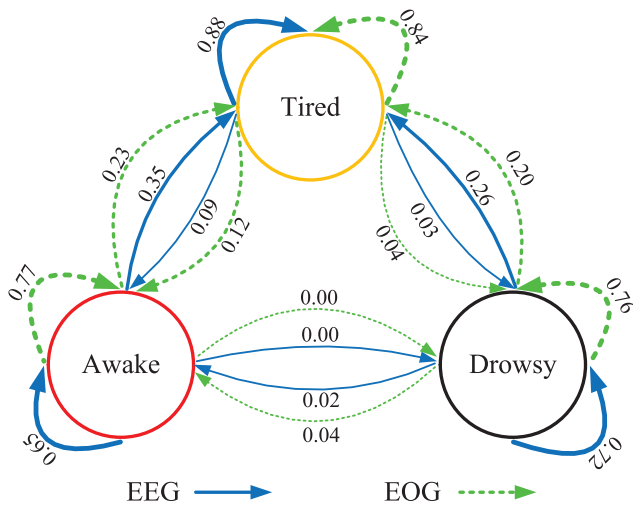


Figure 12. Confusion graph of forehead EOG and posterior EEG, which shows their complementary characteristics for vigilance estimation. Here, the numbers denote the percentage values of samples in the class (arrow tail) classified as the class (arrow head). Bolder lines indicate higher values.

vigilance estimation. Combining the complementary information of these two modalities, modality fusion can improve the prediction performance.

4. Discussion

In this study, we have developed a multimodal approach for vigilance estimation regarding temporal dependency and combining EEG and forehead EOG in a simulated driving environment. The main contributions of this paper are as follows: (1) we have explored the effect of EEG for vigilance estimation in different brain areas: frontal, temporal, and posterior; (2) a multimodal vigilance estimation framework with EEG and forehead EOG has been proposed in terms of feasibility and accuracy; (3) both EEG and EOG signals have been acquired simultaneously with four shared electrodes on the forehead and combined for vigilance estimation; (4) we have revealed the complementary characteristics of EEG and forehead EOG modalities for vigilance estimation; (5) continuous conditional neural field (CCNF) and continuous conditional random field (CCRF) models have been introduced to enhance the performance to capture dynamic temporal dependency; and (6) Neural patterns regarding critical frequency activities under awake and drowsy states have been investigated.

Several researchers have performed pilot studies for on-road real driving tests. Papadelis *et al* designed an on-board system to assess a driver's alertness level in real driving conditions (Papadelis *et al* 2007). They found that EEG and EOG are promising neurophysiological indicators for monitoring sleepiness. Haufe *et al* performed a study to assess the real-world feasibility of EEG-based detection of emergency braking intention (Haufe *et al* 2014). Indeed, in addition to driving applications, there are many other scenarios that require vigilance estimation, such as students' performance in classes. Sievertsen and colleagues examined how cognitive

fatigue influences students' performance on standardized tests in their study (Sievertsen *et al* 2016).

Considering the wearability and feasibility of a vigilance estimation device for real-world applications, we have designed four-electrode placements on the forehead, which are suitable for attachment in a wearable headset or headband. We can collect both EEG and EOG simultaneously and combine their advantages via shared forehead electrodes. The experimental results demonstrate that our proposed approach can achieve comparable performance with the conventional methods on critical brain areas, such as parietal and occipital sites. This approach increases the information flow with easy setups while not considerably increasing the cost.

In recent years, substantial progress has been made in dry electrodes and high-performance amplifiers. Several commercial EEG systems have emerged for increasing the usability in real-world applications (Grozea *et al* 2011, Hairston *et al* 2014, Mullen *et al* 2015). It is feasible to integrate these techniques with our proposed approach to design a new wearable hybrid EEG and forehead EOG system for vigilance estimation in the future.

There are still some limitations for our work, e.g. the age range of subjects in the experiments. All subjects were young adults in the university, which limits the generalization of our approach to other age groups. And in this study, we focus only on vigilance estimation without considering any neuro-feedback. For example, a feedback can be timely provided to the driver to enhance driving safety if the vigilance detection system indicates that he or she is in an extremely tired state. An adaptive closed-loop BCI system that consists of vigilance detection and feedback is very useful in changing environments (Wu *et al* 2010, Lin *et al* 2013). How to efficiently provide and assess the feedback in high vigilance tasks should be further investigated.

Due to individual differences of neurophysiological signals across subjects and sessions, the performance of vigilance estimation models may be dramatically degraded. The generalization performance of vigilance estimation models should be considered for individual differences and adaptability. However, training subject-specific models requires time-consuming calibrations. To address these problems, one efficient approach is to train models on the existing labelled data from a group of subjects and generalize the models to the new subjects with transfer learning techniques (Pan and Yang 2010, Morioka *et al* 2015, Wronkiewicz *et al* 2015, Zhang *et al* 2015b, Zheng and Lu 2016).

5. Conclusion

In this paper, we have proposed a multimodal vigilance estimation approach using EEG and forehead EOG. We have applied different separation strategies to extract VEO_f , HEO_f and EEG signals from four shared forehead electrodes. The COR and RMSE of single forehead EOG-based and EEG-based methods are 0.78/0.12 and 0.70/0.13, respectively, whereas the modality fusion with temporal dependency can significantly enhance the performance with values of 0.85/0.09. The

experimental results have demonstrated the feasibility and efficiency of our proposed approach based on the forehead setup. Our vigilance estimation method has the following three main advantages: both EEG and EOG signals can be acquired simultaneously with four shared electrodes on the forehead; modelling both internal cognitive states and external subconscious behaviours with fusion of forehead EEG and EOG; and introducing temporal dependency to capture the dynamic patterns of the vigilance of users. From the experimental results, we have observed that phenomena of increasing theta and alpha frequency activities and decreasing gamma frequency activities in drowsy states do exist in contrast to awake states. We have also investigated the complementary characteristics of forehead EOG and EEG for vigilance estimation. Our experimental results indicate that the proposed approach can be used to implement a wearable passive brain-computer interface for tasks that require sustained attention.

Acknowledgments

This work was supported in part by grants from the National Natural Science Foundation of China (Grant Nos. 61272248 and 61673266), the National Basic Research Program of China (Grant No. 2013CB329401), the Major Basic Research Program of Shanghai Science and Technology Committee (Grant No. 15JC1400103), and the Technology Research and Development Program of China Railway Corporation (Grant No. 2016Z003-B).

References

- Baltrusaitis T, Banda N and Robinson P 2013 Dimensional affect recognition using continuous conditional random fields *10th IEEE Int. Conf. and Workshops on Automatic Face and Gesture Recognition* (IEEE) pp 1–8
- Baltrušaitis T, Robinson P and Morency L P 2014 *Computer Vision—ECCV* (Springer) pp 593–608
- Bergasa L M, Nuevo J, Sotelo M A, Barea R and Lopez M E 2006 Real-time system for monitoring driver vigilance *IEEE Trans. Intell. Transp. Syst.* **7** 63–77
- Berka C, Levendowski D J, Lumicao M N, Yau A, Davis G, Zivkovic V T, Olmstead R E, Tremoulet P D and Craven P L 2007 EEG correlates of task engagement and mental workload in vigilance, learning, and memory tasks *Aviat. Space Environ. Med.* **78** B231–44
- Bulling A *et al* 2011 Eye movement analysis for activity recognition using electrooculography *IEEE Trans. Pattern Anal. Mach. Intell.* **33** 741–53
- Calvo R A and D’Mello S 2010 Affect detection: an interdisciplinary review of models, methods, and their applications *IEEE Trans. Affective Comput.* **1** 18–37
- Daly I, Scherer R, Billinger M and Muller-Putz G 2015 Force: fully online and automated artifact removal for brain-computer interfacing *IEEE Trans. Neural Syst. Rehabil. Eng.* **23** 725–36
- Damouisis I G and Tzovaras D 2008 Fuzzy fusion of eyelid activity indicators for hypovigilance-related accident prediction *IEEE Trans. Intell. Transp. Syst.* **9** 491–500
- Davidson P R, Jones R D and Peiris M T 2007 EEG-based lapse detection with high temporal resolution *IEEE Trans. Biomed. Eng.* **54** 832–9
- Delorme A and Makeig S 2004 EEGLAB: an open source toolbox for analysis of single-trial EEG dynamics including independent component analysis *J. Neurosci. Methods* **134** 9–21
- Dinges D F and Grace R 1998 PERCLOS: a valid psychophysiological measure of alertness as assessed by psychomotor vigilance *US Department of Transportation, Federal Highway Administration, Publication Number FHWA-MCRT-98-006*
- D’mello S K and Kory J 2015 A review and meta-analysis of multimodal affect detection systems *ACM Comput. Surv.* **47** 43
- Dong Y, Hu Z, Uchimura K and Murayama N 2011 Driver inattention monitoring system for intelligent vehicles: a review *IEEE Trans. Intell. Transp. Syst.* **12** 596–614
- Duan R N, Zhu J Y and Lu B L 2013 Differential entropy feature for EEG-based emotion classification *6th Int. IEEE/EMBS Conf. on Neural Engineering* (IEEE) pp 81–4
- Ferrara M and De Gennaro L 2001 How much sleep do we need? *Sleep Med. Rev.* **5** 155–79
- Gao X Y, Zhang Y F, Zheng W L and Lu B L 2015 Evaluating driving fatigue detection algorithms using eye tracking glasses *7th Int. IEEE/EMBS Conf. on Neural Engineering* (IEEE) pp 767–70
- Grier R A, Warm J S, Dember W N, Matthews G, Galinsky T L, Szalma J L and Parasuraman R 2003 The vigilance decrement reflects limitations in effortful attention, not mindlessness *Human Factors: J. Human Factors Ergon. Soc.* **45** 349–59
- Grozea C, Voinescu C D and Fazli S 2011 Bristle-sensors/low-cost flexible passive dry EEG electrodes for neurofeedback and BCI applications *J. Neural Eng.* **8** 025008
- Hairston W D, Whitaker K W, Ries A J, Vettel J M, Bradford J C, Kerick S E and McDowell K 2014 Usability of four commercially-oriented EEG systems *J. Neural Eng.* **11** 046018
- Haufe S, Kim J W, Kim I H, Sonnleitner A, Schrauf M, Curio G and Blankertz B 2014 Electrophysiology-based detection of emergency braking intention in real-world driving *J. Neural Eng.* **11** 056011
- Haynes J D and Rees G 2006 Decoding mental states from brain activity in humans *Nat. Rev. Neurosci.* **7** 523–34
- Huang R S, Jung T P and Makeig S 2009 *Foundations of Augmented Cognition, Neuroergonomics and Operational Neuroscience* (New York: Springer) pp 394–403
- Huo X Q, Zheng W L and Lu B L 2016 Driving fatigue detection with fusion of EEG and forehead EOG *Int. Joint Conf. on Neural Networks* pp 897–904
- Imbrasaitė V, Baltrusaitis T and Robinson P 2014 CCNF for continuous emotion tracking in music: Comparison with CCRF and relative feature representation *IEEE Int. Conf. on Multimedia and Expo Workshops* (IEEE) pp 1–6
- Jap B T, Lal S, Fischer P and Bekiaris E 2009 Using EEG spectral components to assess algorithms for detecting fatigue *Expert Syst. Appl.* **36** 2352–9
- Ji Q, Zhu Z and Lan P 2004 Real-time nonintrusive monitoring and prediction of driver fatigue *IEEE Trans. Veh. Technol.* **53** 1052–68
- Jung T P, Makeig S, Humphries C, Lee T W, Mckeown M J, Iragui V and Sejnowski T J 2000 Removing electroencephalographic artifacts by blind source separation *Psychophysiology* **37** 163–78
- Kang J S, Park U, Gonuguntla V, Veluvolu K and Lee M 2015 Human implicit intent recognition based on the phase synchrony of EEG signals *Pattern Recognit. Lett.* **66** 144–52
- Khushaba R N, Kodagoda S, Lal S and Dissanayake G 2011 Driver drowsiness classification using fuzzy wavelet-packet-based feature-extraction algorithm *IEEE Trans. Biomed. Eng.* **58** 121–31
- Kim I H, Kim J W, Haufe S and Lee S W 2014 Detection of braking intention in diverse situations during simulated driving based on EEG feature combination *J. Neural Eng.* **12** 016001

- Lafferty J, McCallum A and Pereira F C 2001 Conditional random fields: probabilistic models for segmenting and labeling sequence data *18th Int. Conf. on Machine Learning (Morgan Kaufmann)* pp 282–9
- Lee E C, Woo J C, Kim J H, Whang M and Park K R 2010 A brain-computer interface method combined with eye tracking for 3D interaction *J. Neurosci. Methods* **190** 289–98
- Lin C T, Chuang C H, Huang C S, Tsai S F, Lu S W, Chen Y H and Ko L W 2014 Wireless and wearable EEG system for evaluating driver vigilance *IEEE Trans. Biomed. Circuits Syst.* **8** 165–76
- Lin C T, Huang K C, Chao C F, Chen J A, Chiu T W, Ko L W and Jung T P 2010 Tonic and phasic EEG and behavioral changes induced by arousing feedback *NeuroImage* **52** 633–42
- Lin C T, Huang K C, Chuang C H, Ko L W and Jung T P 2013 Can arousing feedback rectify lapses in driving? Prediction from EEG power spectra *J. Neural Eng.* **10** 056024
- Lu Y, Zheng W L, Li B and Lu B L 2015 Combining eye movements and EEG to enhance emotion recognition *Int. Joint Conf. on Artificial Intelligence* pp 1170–6
- Makeig S and Inlow M 1993 Lapse in alertness: coherence of fluctuations in performance and EEG spectrum *Electroencephalogr. Clin. Neurophysiol.* **86** 23–35
- Martel A, Dähne S and Blankertz B 2014 EEG predictors of covert vigilant attention *J. Neural Eng.* **11** 035009
- Ma J X, Shi L C and Lu B L 2010 Vigilance estimation by using electrooculographic features *Annual Int. Conf. of the IEEE Engineering in Medicine and Biology Society (IEEE)* pp 6591–4
- Ma J X, Shi L C and Lu B L 2014 An EOG-based vigilance estimation method applied for driver fatigue detection *Neurosci. Biomed. Eng.* **2** 41–51
- McMullen D P *et al* 2014 Demonstration of a semi-autonomous hybrid brain-machine interface using human intracranial eeg, eye tracking, and computer vision to control a robotic upper limb prosthetic *IEEE Trans. Neural Syst. Rehabil. Eng.* **22** 784–96
- Morioka H, Kanemura A, Hirayama J I, Shikauchi M, Ogawa T, Ikeda S, Kawanabe M and Ishii S 2015 Learning a common dictionary for subject-transfer decoding with resting calibration *NeuroImage* **111** 167–78
- Mühl C, Jeunet C and Lotte F 2014 EEG-based workload estimation across affective contexts *Frontiers Neurosci.* **8**
- Mullen T R, Kothe C A, Chi Y M, Ojeda A, Kerth T, Makeig S, Jung T P and Cauwenberghs G 2015 Real-time neuroimaging and cognitive monitoring using wearable dry EEG *IEEE Trans. Biomed. Eng.* **62** 2553–67
- Nicolaou M *et al* 2011 Continuous prediction of spontaneous affect from multiple cues and modalities in valence-arousal space *IEEE Trans. Affective Comput.* **2** 92–105
- O’Connell R G, Dockree P M, Robertson I H, Bellgrove M A, Foxe J J and Kelly S P 2009 Uncovering the neural signature of lapsing attention: electrophysiological signals predict errors up to 20 s before they occur *J. Neurosci.* **29** 8604–11
- Oken B S and Salinsky M C 2007 Sleeping and driving: not a safe dual-task *Clin. Neurophysiol.* **118** 1899
- Pan S J and Yang Q 2010 A survey on transfer learning *IEEE Trans. Knowl. Data Eng.* **22** 1345–59
- Papadelis C, Chen Z, Kourtidou-Papadeli C, Bamidis P D, Chouvarda I, Bekiaris E and Maglaveras N 2007 Monitoring sleepiness with on-board electrophysiological recordings for preventing sleep-deprived traffic accidents *Clin. Neurophysiol.* **118** 1906–22
- Peiris M T, Davidson P R, Bones P J and Jones R D 2011 Detection of lapses in responsiveness from the EEG *J. Neural Eng.* **8** 016003
- Peng J, Bo L and Xu J 2009 Conditional neural fields *Advances in Neural Information Processing Systems* pp 1419–27
- Pfurtscheller G, Allison B Z, Bauernfeind G, Brunner C, Escalante T S, Scherer R, Zander T O, Mueller-Putz G, Neuper C and Birbaumer N 2010 The hybrid BCI *Frontiers Neurosci.* **4** 3
- Ranney T A 2008 Driver distraction: a review of the current state-of-knowledge *Technical Report* National Highway Traffic Safety Administration, Washington, DC, USA
- Ray W J and Cole H W 1985 EEG alpha activity reflects attentional demands, and beta activity reflects emotional and cognitive processes *Science* **228** 750–2
- Rosenberg M D, Finn E S, Scheinost D, Papademetris X, Shen X, Constable R T and Chun M M 2016 A neuromarker of sustained attention from whole-brain functional connectivity *Nat. Neurosci.* **19** 165–71
- Sahayadhas A, Sundaraj K and Murugappan M 2012 Detecting driver drowsiness based on sensors: a review *Sensors* **12** 16937–53
- Shi L C, Jiao Y Y and Lu B L 2013 Differential entropy feature for EEG-based vigilance estimation *35th Annual Int. Conf. of the IEEE Engineering in Medicine and Biology Society (IEEE)* pp 6627–30
- Shi L C and Lu B L 2010 Off-line and on-line vigilance estimation based on linear dynamical system and manifold learning *Annual Int. Conf. of the IEEE Engineering in Medicine and Biology Society (IEEE)* pp 6587–90
- Shi L C and Lu B L 2013 EEG-based vigilance estimation using extreme learning machines *Neurocomputing* **102** 135–43
- Sievertsen H H, Gino F and Povesan M 2016 Cognitive fatigue influences students performance on standardized tests *Proc. Natl Acad. Sci.* **113** 2621–4
- Trutschel U, Sirois B, Sommer D, Golz M and Edwards D 2011 PERCLOS: an alertness measure of the past *Driving Assess.* **2011** 6th
- Urigüen J A and Garcia-Zapirain B 2015 EEG artifact removal state-of-the-art and guidelines *J. Neural Eng.* **12** 031001
- Wang Y K, Jung T P and Lin C T 2015 EEG-based attention tracking during distracted driving *IEEE Trans. Neural Syst. Rehabil. Eng.* **23** 1085–94
- Wronkiewicz M, Larson E and Lee A K 2015 Leveraging anatomical information to improve transfer learning in brain-computer interfaces *J. Neural Eng.* **12** 046027
- Wu D, Courtney C G, Lance B J, Narayanan S S, Dawson M E, Oie K S and Parsons T D 2010 Optimal arousal identification and classification for affective computing using physiological signals: virtual reality stroop task *IEEE Trans. Affective Comput.* **1** 109–18
- Zander T O and Jatzev S 2012 Context-aware brain-computer interfaces: exploring the information space of user, technical system and environment *J. Neural Eng.* **9** 016003
- Zander T O and Kothe C 2011 Towards passive brain-computer interfaces: applying brain-computer interface technology to human-machine systems in general *J. Neural Eng.* **8** 025005
- Zhang Y F, Gao X Y, Zhu J Y, Zheng W L and Lu B L 2015a A novel approach to driving fatigue detection using forehead EOG *7th Int. IEEE/EMBS Conf. on Neural Engineering (IEEE)* pp 707–10
- Zhang Y Q, Zheng W L and Lu B L 2015b Transfer components between subjects for EEG-based driving fatigue detection *Int. Conf. on Neural Information Processing (New York: Springer)* pp 61–8
- Zheng W L, Dong B N and Lu B L 2014 Multimodal emotion recognition using EEG and eye tracking data *36th Annual Int. Conf. of the IEEE Eng. in Medicine and Biology Society (IEEE)* pp 5040–3
- Zheng W L and Lu B L 2015 Investigating critical frequency bands and channels for EEG-based emotion recognition with deep neural networks *IEEE Trans. Auton. Mental Dev.* **7** 162–75
- Zheng W L and Lu B L 2016 Personalizing EEG-based affective models with transfer learning *Int. Joint Conf. on Artificial Intelligence* pp 2732–8